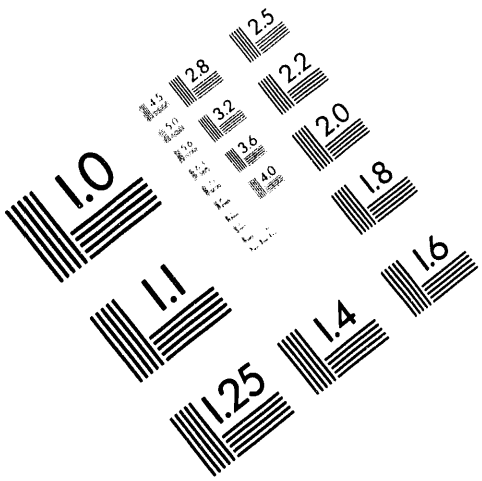

Association for Information and Image Management
1100 Wayne Avenue, Suite 1100
Silver Spring, Maryland 20910
301/587-8202

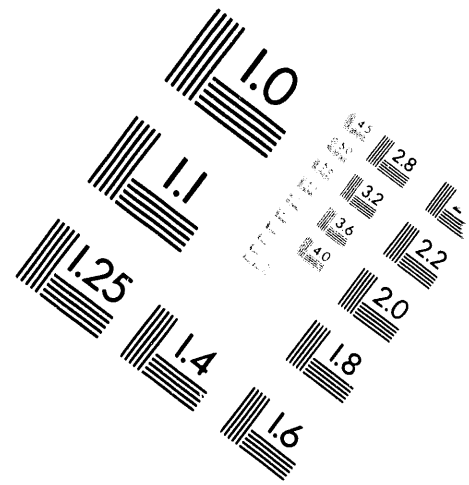

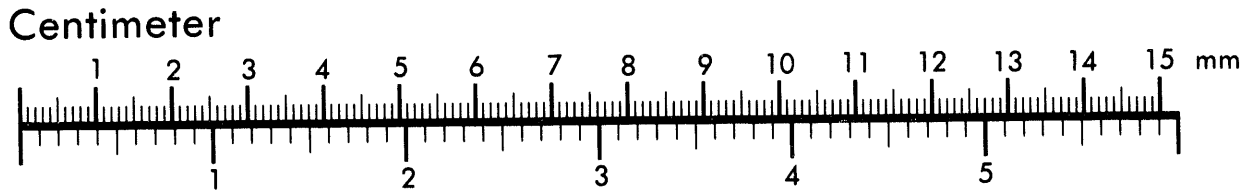

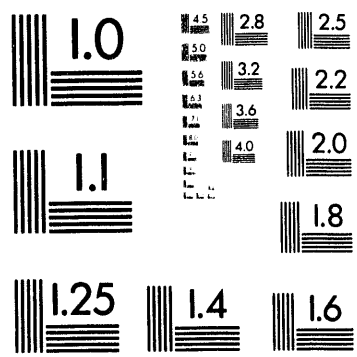

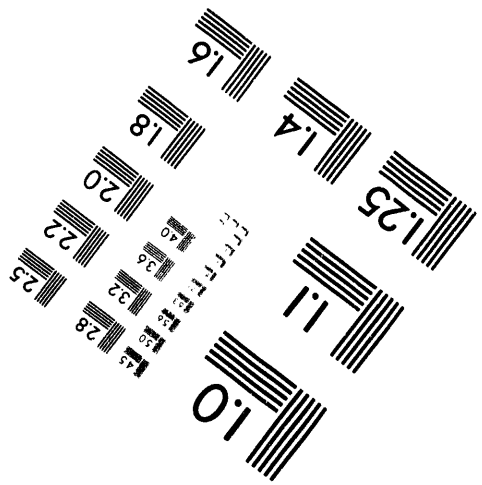

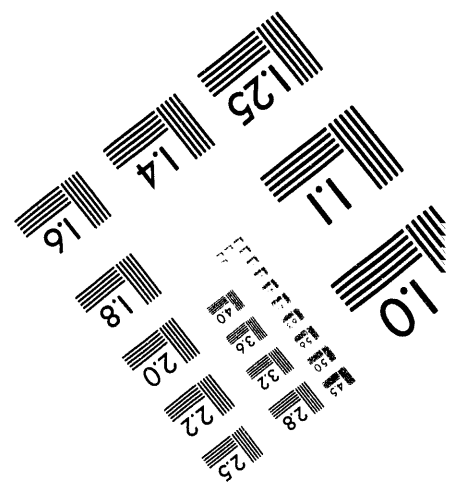

1 of 1

Conf-9410165--2

LA-UR-94-2574

Title: Rietveld Refinement of Magnetic Structures from Pulsed-Neutron-Source Powder-Diffraction Data

Author(s): R. A. Robinson, A. C. Lawson, A. C. Larson, R. B. Von Dreele, J. A. Goldstone

Submitted to: International Conference on Neutron Scattering, Sendai, Japan, 11-14 October 1994; To be published in Physica B

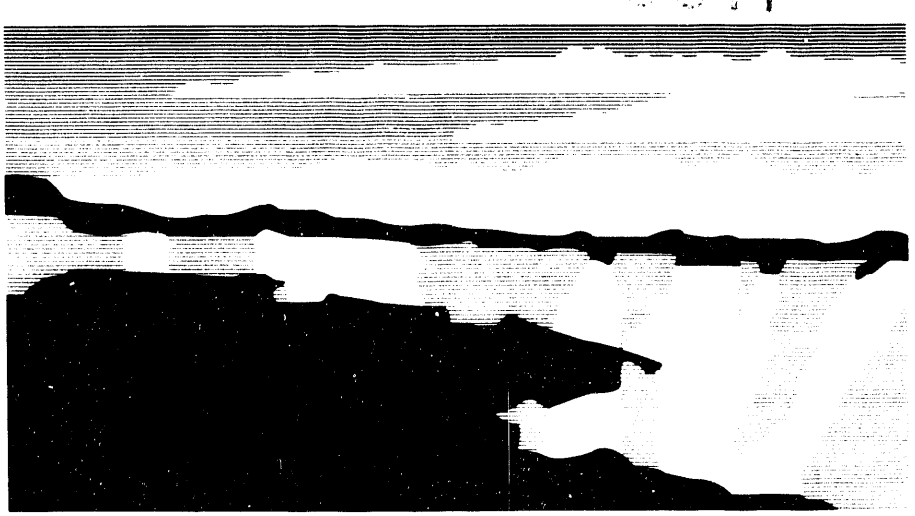

Los Alamos
NATIONAL LABORATORY

Form No. 836 R5
ST 2629 10/91

Rietveld Refinement of Magnetic Structures from Pulsed-Neutron-Source Powder-Diffraction Data

R. A. Robinson, A. C. Lawson, Allen C. Larson, R. B. Von Dreele and J. A. Goldstone
LANSCE, Los Alamos National Laboratory, Los Alamos, NM 87545.

The General Structure Analysis System, GSAS, has recently been modified to include magnetic neutron-scattering cross-sections. Low-temperature diffraction data have been taken on the hexagonal noncollinear antiferromagnet UPdSn on both the HIPD and the NPD powder diffractometers at LANSCE. The low-resolution data reveal that the magnetic structure has orthorhombic symmetry (magnetic space group $P_Cm'c2_1$) between 25K and 40K, and monoclinic symmetry (magnetic space group P_C112_1) below 25K. The high-resolution data reveal that there are structural distortions with corresponding symmetry changes in each of these phases, to give chemical space groups $Cmc2_1$ and $P2_1$ respectively, while the paramagnetic phase above 40K has space group $P6_3mc$. Using GSAS, we have refined data sets from both diffractometers simultaneously, including both magnetic and structural cross-sections. Magnetoelastic coefficients for the distortions have been extracted and we have determined the sign of the coupling between the structural monoclinicity and the magnetic monoclinicity. The magnetic results from Rietveld refinement are in good agreement with model fitting to the integrated intensities of seven independent magnetic reflections and these, in turn, agree with measurements made on the same sample using the constant-wavelength reactor technique. Our results therefore validate, to some level, both the technique of using spallation sources for complicated magnetic structures and the specifics of the GSAS Rietveld code.

Keywords: Rietveld Refinement, Magnetic Powder Diffraction, UPdSn
Responsible Author: R. A. Robinson, LANSCE, Mail Stop H805, Los Alamos National Laboratory, Los Alamos, NM 87545, USA., FAX: 505-665-2676, e-mail: RROBINSON@LANL.GOV

1. Introduction

It is now fifteen years or so since accelerator-based pulsed spallation neutron sources proved themselves useful scientific tools in materials science and condensed matter physics. The most immediate success was in high-resolution neutron powder diffraction, using moderators with sharp timing pulses and detector arrays almost in backscattering. The backscattering arrangement automatically gives excellent resolution, and almost a decade in d-spacing range (typically from 0.4 to 3 Å) can be covered easily using room temperature moderators. Wavelength is scanned (by time-of-flight) at fixed scattering angle. In contrast, apart from one early study of FeGe[1], very little *magnetic* powder diffraction work was performed and until recently this field remained the preserve of the constant-wavelength technique at research reactors. The most striking example of this was that, while the crystallographic structures of high-T_C materials were initially determined[2] using pulsed neutrons at IPNS, the long-range antiferromagnetic order in La_2CuO_{4-y} was observed somewhat later using the constant-wavelength technique at the Brookhaven reactor[3].

The technical reason for this is not that spallation sources are unsuited to magnetic studies - the cross sections are, of course, the same at both sources. Rather, the trick of working in backscattering makes pulsed sources so good for high-resolution crystallographic studies that they have concentrated in this area. Magnetic diffraction experiments rarely require such high resolution, are often intensity limited, and the data of interest often lie at longer d-spacings (typically 2-10Å). Therefore, if one is to remain in backscattering, the spectrometer should view a cold neutron source. Alternatively, lower angle detector banks are required. The experiment is also done in a different way: as wavelength is the scanning variable, rather than 2θ, there was some concern that one could not make all the wavelength-dependent corrections (absorption, extinction etc.) properly. Finally, while magnetic cross-sections were included in Rietveld's original constant-wavelength program[4], they have only recently been incorporated into the Rietveld programs like GSAS[5-7] that can handle time-of-flight data.

In the mean time a variety of magnetic neutron powder diffraction studies were performed at LANSCE [8-12] and at ISIS [13,14] using peak-by-peak extraction of integrated intensities, to which the magnetic structure model was fitted. In particular, the study[11] on HIPD[12] at LANSCE of Bi_2CuO_4 showed, in a system very much like the High-Tc superconductors, that moments of order $0.5\mu_B$ can be seen just as easily at pulsed sources, so long as detectors at low scattering angles (40^o in this case) are used.

The powerful Rietveld refinement package GSAS[5] has a number of distinctive features. Firstly, it can handle multiple data sets. At LANSCE, we routinely co-refine data taken in 6 banks (at $\pm 153^{o}$, $\pm 90^{o}$ and $\pm 40^{o}$) on HIPD[12]. Indeed, as we show later in this paper, joint refinements with up to ten banks of data from two different spectrometers have been performed. Likewise, X-ray and neutron data can been combined in one refinement[15]. Though it has not been done yet, reactor and spallation source data on the same sample could be co-refined, as could data taken on two reactor diffractometers with differing resolutions and d-spacing ranges. In 1991, magnetic cross-sections were included in GSAS[6], and the first successful magnetic Rietveld refinement at a pulsed spallation source was published the following year[16,17]. Since then, a large number of studies have been performed. In the rest of this article, we concentrate on our own study of the noncollinear hexagonal antiferromagnet UPdSn, which is of interest for a number of reasons. Firstly, it is part of a broader program to understand the role of hybridisation of 5f electrons with ligand d electrons in uranium magnetic moment formation. Secondly, the uranium ions lie on a simple hexagonal lattice, at least above the magnetic ordering temperature T_N = 37K, so it is an ideal hexagonal antiferromagnet. Thirdly, in the course of our studies, we have checked the GSAS Rietveld refinement against peak-by-peak analysis of the same data, and have compared the spallation-source intensities against constant-wavelength data taken on the same sample at a reactor. We find good agreement in both cases, and therefore believe we have validated both the technique of using spallation sources for complicated magnetic structures and the specifics of the GSAS Rietveld code.

2. An example: Magnetic Order and Structural Distortions in UPdSn

We have had an extensive program to study the noncollinear hexagonal antiferromagnet UPdSn using both powder[18-20] and single-crystal[21-23] neutron techniques at the LANSCE spallation source and the NIST reactor. In our initial low-resolution powder work[18], we showed that the Pd and Sn atoms were chemically ordered and that the space group was $P6_3mc$. In addition we showed that there were probably two magnetic phases, one with orthorhombic magnetic symmetry between 23 and 37K and a second related monoclininc magnetic phase below 23K. Portions of our original 40^{o} powder data are shown in Figure 1. The indexing is in a double-sized orthorhombic cell, as shown in Figure 2. From Figure 1(b) and (c), we were able to deduce the orthorhombic magnetic structure (for $23K < T < 37K$) shown in Figure 2(a) and tabulated in Table 1.

The reasoning for this intermediate structure is as follows: (1) Note that all observed magnetic reflections have $h+k$ odd. This necessarily implies that the magnetic structure is *anticentred.* i.e. the moment at 0,0,1/4 is antiparallel to that at 1/2,1/2,1/4, and likewise for the two uranium ions at z = 3/4. (2) Note that reflections with l odd are observed. As reasoned in Ref. 18, this means that the magnetic structure must be *noncollinear.* (3) Between 23 and 37K, the 010 magnetic reflection is systematically absent. Therefore the net moment on each (010) plane, which is carried by two uranium ions at 0,0,±1/4, must be parallel to the [010] axis. These two atoms are on crystallographically equivalent sites and should carry the same moment. Therefore, they should have μ_y parallel to each other, but the μ_x and μ_z components should be antiparallel on the two sites. This ensures that the vector sum of the moments on the two sites lies parallel to [010]. (4) The uranium atoms lie in a mirror plane perpendicular to the x axis. Including time reversal symmetry, or not, this becomes an antimirror plane (symmetry element m') or mirror plane (symmetry element m). In the second case, the moments would be purely perpendicular to the plane, giving a collinear structure, which we already know to be incorrect from point (2) above. Alternatively, with the antimirror plane, the moments must lie in the y-z plane. That is, the four atoms at (0,0,±1/4)±(1/2,1/2,0) have the arrangement of cartesian moments given in Table I(a), and shown on Figure 1(a). This phase has orthorhombic symmetry (Shubnikov group $P_Cm'c2_1$) and with the reasoning given above this is a unique solution.

The next step is to derive the magnetic structure below 23K. The most prominent feature of the data below 23K, shown in Figure 1, is the development of the 010 magnetic reflection. There is only one remaining degree of freedom with which to explain these data, namely the addition of an x-component to the moment. There are three independent ways of arranging such components on the 4 sites, but only one of these gives a non-zero intensity on the 010 reflection. This is also the only permutation that preserves the anticentring symmetry described above. This model is shown in Figure 2(b) and it gives good agreement with the data. It has monoclinic symmetry (Shubnikov group P_C112_1)

The fact that the magnetic symmetry is orthorhombic between 23K and 37K, and monoclinic below 23K means that there should in principle be structural distortions with those symmetries in the same temperature ranges. These have been observed and characterised in an experiment[20] on the same sample using the high-resolution powder diffractometer NPD at LANSCE. NPD currently has detector banks at $\pm148^\circ$ and $\pm90^\circ$, with $\Delta d/d$ resolutions of 0.15% and 0.25% respectively. Representative data are shown in Fig. 3. In this study, we were even able to measure the sign of the coupling between the monoclinic distortion (γ-90)

and the "magnetic monoclinicity", μ_x. The data taken on NPD were co-refined with the previous data taken on HIPD, and the full patterns are shown, along with markers and residuals, in Figure 3. The parameters for this particular refinement are given in Table 2 of Ref. 20.

3. How to use GSAS[5] for magnetic problems[7]

The GSAS refinement shown in Figure 3 includes the magnetic cross-sections. While this particular example is of spallation-source data, GSAS can equally well be used for refinement of constant-wavelength reactor data. In either case the procedure is the same: (1) Magnetic structures can be tackled either as an extra purely magnetic phase, or as a phase that gives both nuclear and magnetic intensity. (2) In either case, GSAS handles the magnetic symmetry in terms of magnetic Shubnikov space groups which are extensions of the regular crystallographic space groups. The regular space group is defined in GSAS in terms of up to four independent symmetry operators and each of these can be coloured either *black* (with time-reversal symmetry) or *red* (with time-reversal anti-symmetry). But first one must tell GSAS that the phase is magnetic, in the normal space-group section. (3) Then, one moves to the atom-editing section of the least-squares option in order to make each symmetry element red or black and therby specify the Shubmikov group. GSAS automatically determines constraints on the moment components. The systematic absences (as used in the reflection generator POWPREF), however, are calculated by a numerical sampling method. (4) Finally one needs a magnetic form factor and this is parameterised in the following way[24]:

$$F(Q) = \sum_i a_i e^{-b_i Q^2} + C \qquad (1)$$

where a_i, b_i and C are constants which can be fitted in GSAS to published experimental or theoretical form factors in the form of a user-supplied data file, and where $Q = \sin\theta/\lambda$. This is handled in the form-factor section of the least-squares option in GSAS.

4. Discussion

Our original intensity analysis[18] was done using individual integrated intensities. These agree well with integrated intensities measured at the NIST reactor using the constant-wavelength technique[19]. The same data have been used in the Rietveld refinement[20] shown in Figure 3, and again there is good agreement regarding the extracted moments. So

we have confidence that all wavelength-dependent corrections are being applied properly. This is a fairly stringent test, given the noncollinear nature of the magnetic order, and three independent components of the moment. Our results therefore validate, to some level, both the technique of using spallation sources for complicated magnetic structures and the specifics of the GSAS Rietveld code.

Acknowledgements

This work was supported in part by the division of Basic Energy Sciences of the U.S. Department of Energy.

References

[1] G. P. Felcher, J. D. Jorgensen and R. Wäppling, J. Phys. C 16, 6281 (1983).

[2] J. D. Jorgensen, H. -B. Schuttler, D. G. Hinks, D. W. Capone, K. Zhang, M. B. Brodsky and D. J. Scalapino, Phys. Rev. Lett. 58, 1371 (1987).

[3] S. K. Sinha, D. Vaknin, M. S. Alvarez, A. J. Jacobson, J. Newsam, J. T. Lewandowski, D. C. Johnston, C. Stassis, J. M. Tranquada, T. Freltoft, H. Moudden, A. I. Goldman, P. Zolliker, D. E. Cox and G. Shirane, Physica B 156 &157, 854 (1989) and references therein.

[4] H. M. Rietveld, J. Appl. Cryst. 2, 65 (1969). [also Acta Cryst. 22, 151 (1969)].

[5] A. C. Larson and R. B. Von Dreele, Los Alamos National Laboratory Report LA-UR-86-748 (1986).

[6] M. Yethiraj, A. C. Larson and R. B. Von Dreele, private communication.

[7] R. A. Robinson, A. C. Lawson, A. C. Larson, R. B. Von Dreele and J. A. Goldstone, in Proceedings of ICANS-XII, Abingdon, U.K. 24-28 May 1993, Rutherford Appleton Laboratory Report 94-025, Vol. I, p.273-282.

[8] A. C. Lawson, A. Williams, J. L. Smith, P. A. Seeger, J. A. Goldstone, J. A. O'Rourke and Z. Fisk, J. Magn. Magn. Mater. 50, 83 (1985).

[9] A. C. Lawson, A. Williams, J. G. Huber and R. B. Roof, J. Less-Common Met. 120, 113 (1986)

[10] A. C. Lawson, A. Williams and J. G. Huber, J. Less-Common Met. 120, 147 (1986)

[11] E. W. Ong, G. H. Kwei, R. A. Robinson, B. L. Ramakrishna and R. B. Von Dreele, Phys. Rev. B42, 4255 (1990).

[12] A. C. Lawson, J. A. Goldstone, J. G. Huber, A. L. Giorgi, J. W. Conant, A. Severing, B. Cort and R. A. Robinson, J. Appl. Phys. 69, 5112 (1991).

[13] R. Chakravarthy, L. Madhav Rao, S. K. Paranjpe, S. K. Kulshreshtra, A. K. Soper and W. S. Howells, J. de Physique de Colloque 49, C8, 1111 (1988).

[14] R. Chakravarthy, S. K. Paranjpe, S. K. Kulshreshtra, L. Madhav Rao, A. K. Soper and W. S. Howells, J. de Physique Colloque 49, C8, 1113 (1988).

[15] G. H. Kwei, R. B. Von Dreele, A. Wiliams, J. A. Goldstone, A. C. Lawson and W. K. Warburton, J. Molec. Structure 223, 383 (1990).

[16] J. K. Warner, A. K. Cheetham, A. G. Nord, R. B. Von Dreele and M. Yethiraj, J. Mater. Chem. 2, 191 (1992).

[17] J. K. Warner, A. K. Cheetham, D. E. Cox and R. B. Von Dreele, J. Am. Chem. Soc. 114, 6074 (1992).

[18] R. A. Robinson, A. C. Lawson, K. H. J. Buschow, F. R. de Boer, V. Sechovsky and R. B. Von Dreele, J. Magn. Magn. Mater. 98, 147 (1991).

[19] R. A. Robinson, A. C. Lawson, J. W. Lynn and K. H. J. Buschow, Phys. Rev. B45, 2939 (1992).

[20] R. A. Robinson, A. C. Lawson, J. A. Goldstone and K. H. J. Buschow, J. Magn. Magn. Mater. 128, 143 (1993).

[21] H. Nakotte, R. A. Robinson, J. W. Lynn, E. Brück and F. R. de Boer, Phys. Rev. B47, 831 (1993).

[22] S. W. Johnson, R. A. Robinson, H. Nakotte, E. Brück, F. R. de Boer and A. C. Larson, J. Appl. Phys. 73, 6072 (1993).

[23] R. A. Robinson, J. W. Lynn, A. C. Lawson and H. Nakotte, J. Appl. Phys. 75, 6589 (1994).

[24] This is the same mathematical form as given for the $\langle j_0 \rangle$ magnetic form factors tabulated by P. J. Brown, in International Tables for Crystallography, ed. A. J. C. Wilson (Kluwer, Dordrecht, 1992), Vol. C, p. 391ff.

Table 1 Components of the magnetic moments on the four uranium atoms in the orthorhombic magnetic cell

Uranium atom position **r**	Magnetic Phase I (23K<T<37K)	Magnetic Phase II (T<23K)
0,0,1/4	$0,\mu_y,\mu_z$	μ_x,μ_y,μ_z
0,0,-1/4	$0,\mu_y,-\mu_z$	$\mu_x,\mu_y,-\mu_z$
1/2,1/2,1/4	$0,-\mu_y,-\mu_z$	$-\mu_x,-\mu_y,-\mu_z$
1/2,1/2,-1/4	$0,-\mu_y,\mu_z$	$-\mu_x,-\mu_y,\mu_z$

Figure Captions

Figure 1. Plot of a portion of raw data taken in the $+40^{o}$ bank of HIPD at 4 temperatures: (a) at 13K in the monoclinic magnetic phase II, (b) and (c) at 33.8 and 36.3K respectively in orthorhombic magnetic phase I, and (d) at 46K in the hexagonal paramagnetic state. The indices in the upper panel are for the magnetic reflections only, assuming the orthorhombic magnetic cell shown in Fig. 2. The intensities have been divided by the incident spectrum. (after Ref. 18)

Figure 2. The magnetic structures of UPdSn: (a) in orthorhombic magnetic phase I for $23 < T < 37$K, and (b) in monoclinic magnetic phase II for $T < 23$K. In each case the right-hand figure shows the projection onto the orthorhombic a,b-plane, which is the same as the hexagonal basal plane shown by the dashed lines. The left-hand figures show projections onto the orthorhombic b,c-plane. For purposes of clarity, only the uranium atoms and moments are shown (after Figs. 4 and 5 in Ref. 18 and Fig. 5 in Ref. 20)

Figure 3. Plots of the 110 hexagonal reflection in UPdSn as a function of temperature, taken on the $+148^{o}$ bank of NPD. The splittings are indexed in the orthorhombic system at 32K and in the monoclinic system below that. The intensities have been divided by the incident spectrum. (after Ref. 20)

Figure 4. The 10-bank joint Rietveld refinement including magnetism of UPdSn at 14K, as described in the text (5 banks, only half the data, are displayed here). The refinement is in space group $C112_1$, with magnetic space group P_C112_1 and fitted parameters as given in Table 2 of Ref. 20. (a) NPD $2\theta=148^{o}$ with resolution $\Delta d/d = 0.15\%$, (b) NPD $2\theta=90^{o}$ with resolution $\Delta d/d = 0.25\%$, (c) HIPD $2\theta=153^{o}$ with resolution $\Delta d/d = 0.7\%$, (d) HIPD $2\theta=90^{o}$ with resolution $\Delta d/d = 1.1\%$, (e) HIPD $2\theta=40^{o}$ with resolution $\Delta d/d = 1.8\%$. The reflection marked by the asterisk in the middle top panel is the same data as in Fig. 3(f). The range shown by the arrows in the bottom panel is the same data as in Fig. 1(a) The ordinate scale is piecewise linear and each row of panels is on the same intensity scale. The intensities have been divided by the incident spectrum.

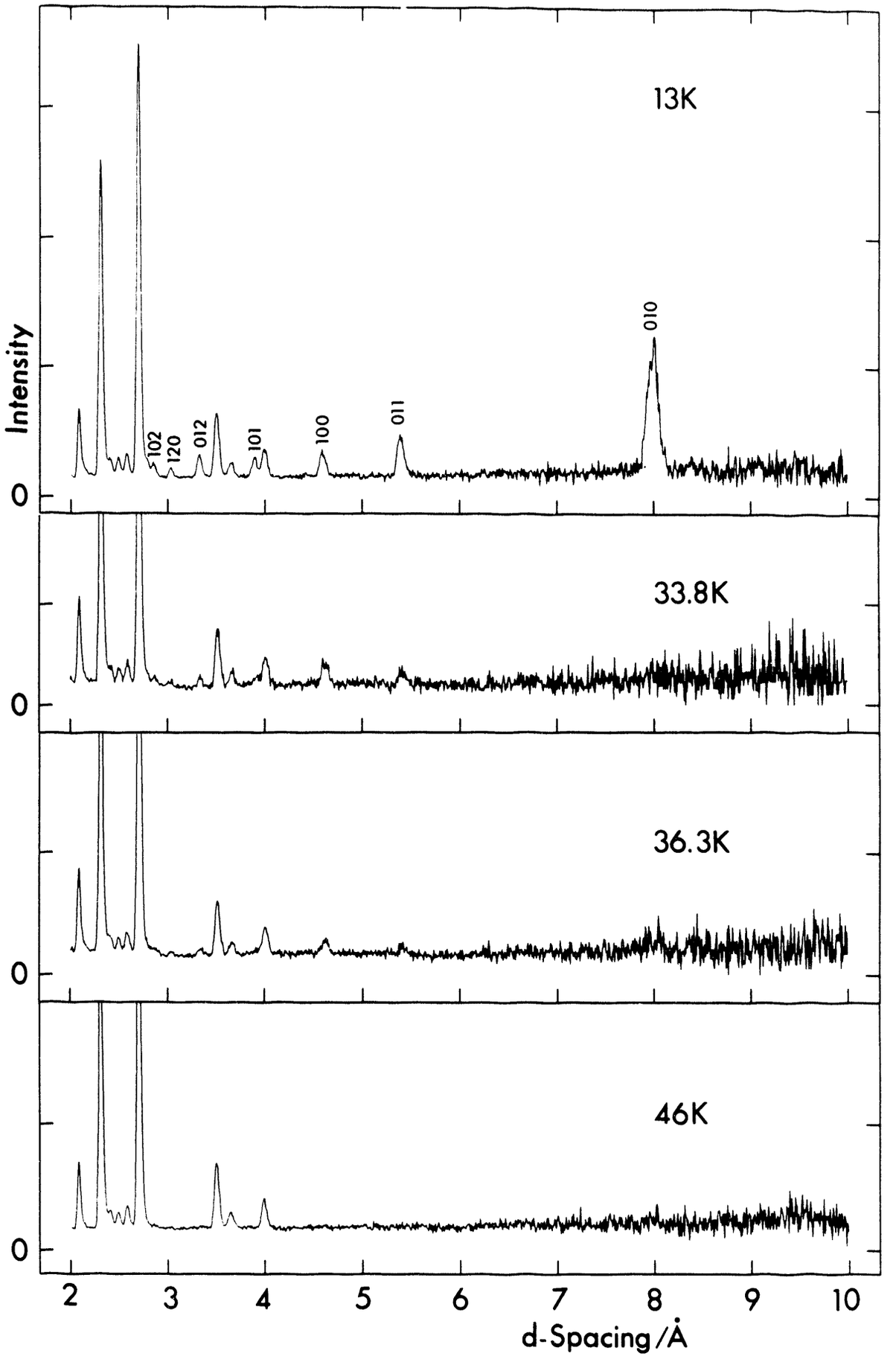
13K
33.8K
36.3K
46K
Intensity
0
102
120
012
101
100
011
010
2
3
4
5
6
7
8
9
10
d-Spacing /Å

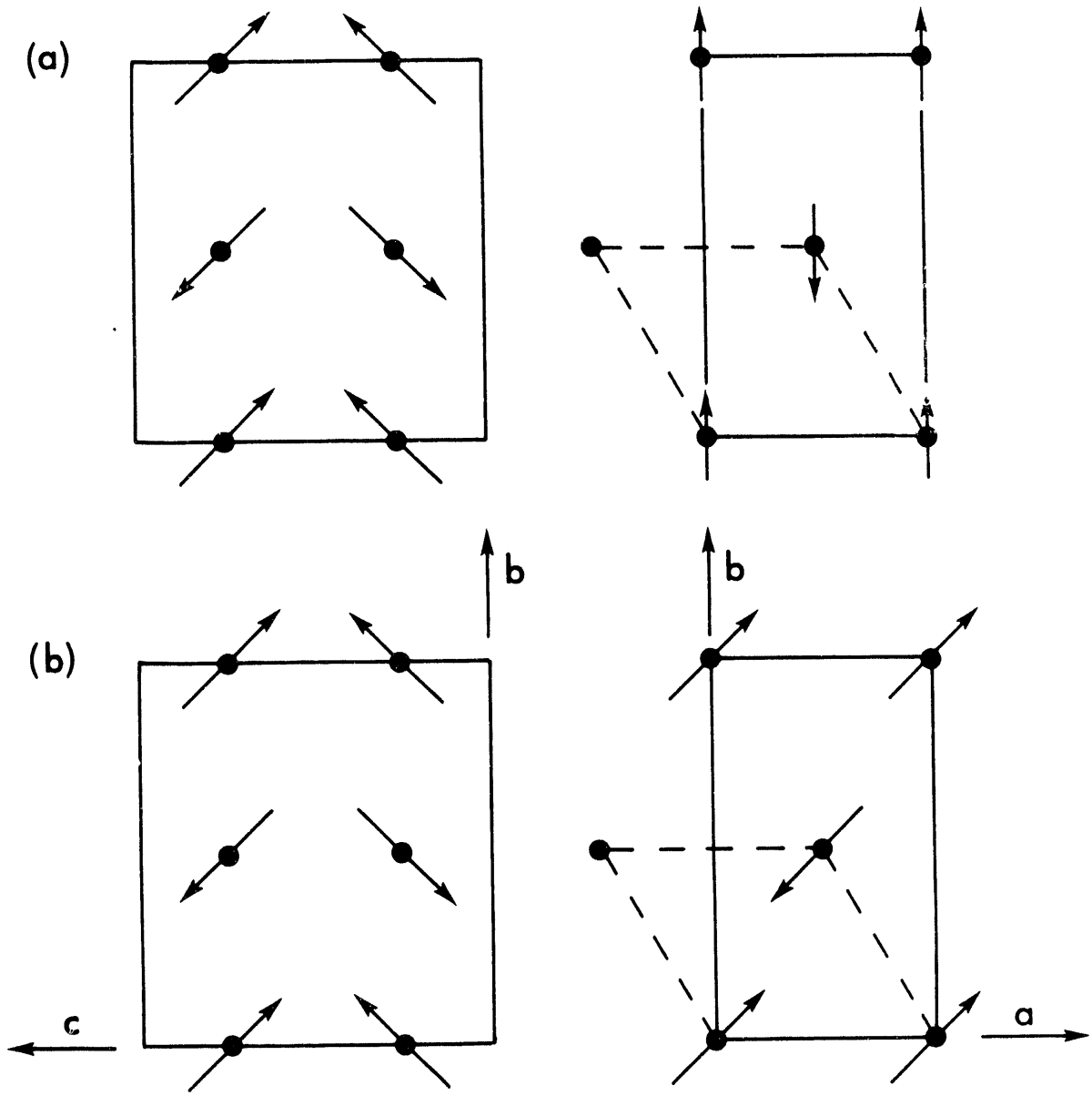
(a)
(b)
b
b
c
a

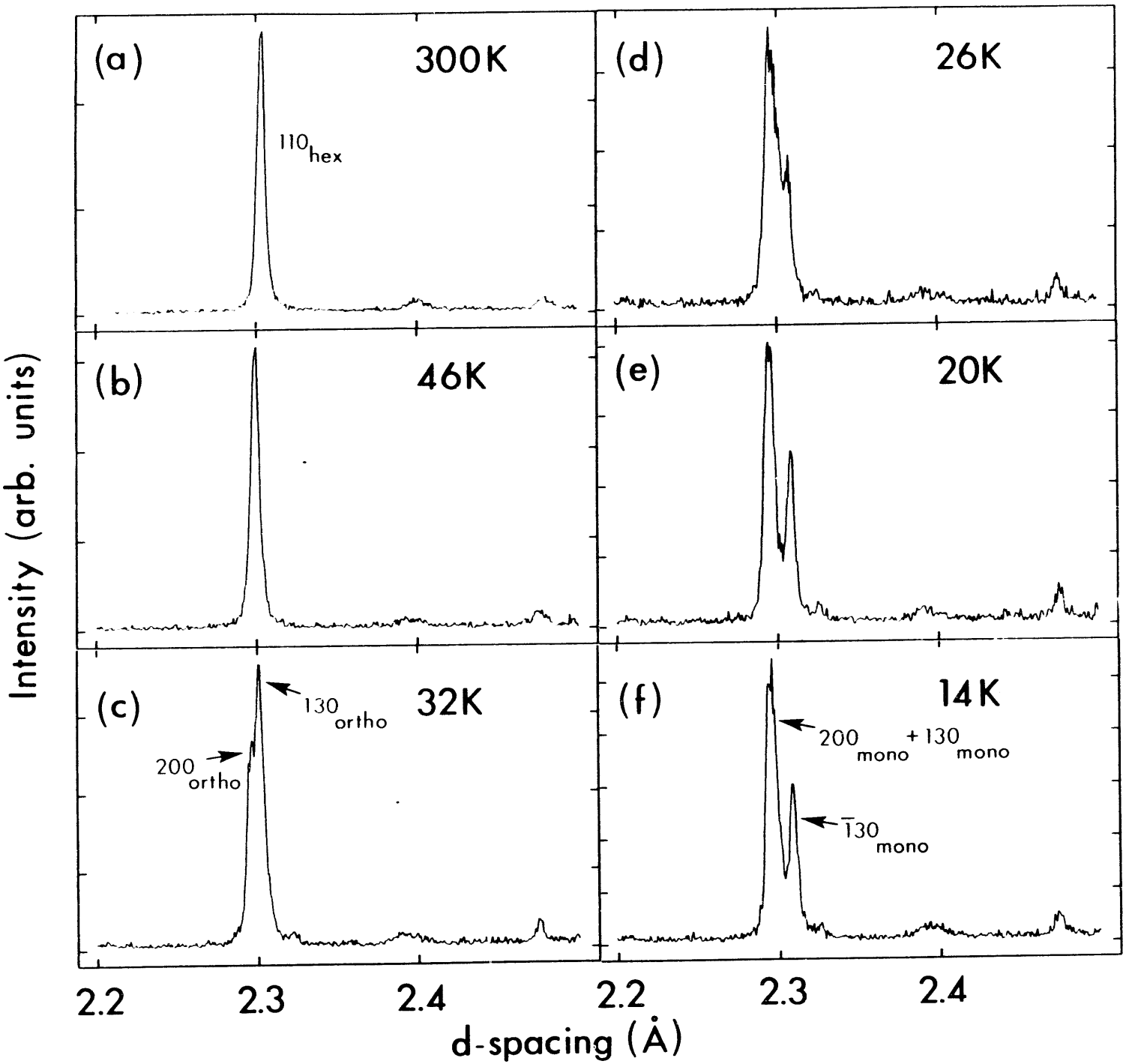
(a)
300K
110_{hex}
(d)
26K
(b)
46K
(e)
20K
(c)
32K
130_{ortho}
200_{ortho}
(f)
14K
$200_{mono} + 130_{mono}$
$\bar{1}30_{mono}$
Intensity (arb. units)
2.2
2.3
2.4
2.2
2.3
2.4
d-spacing (Å)

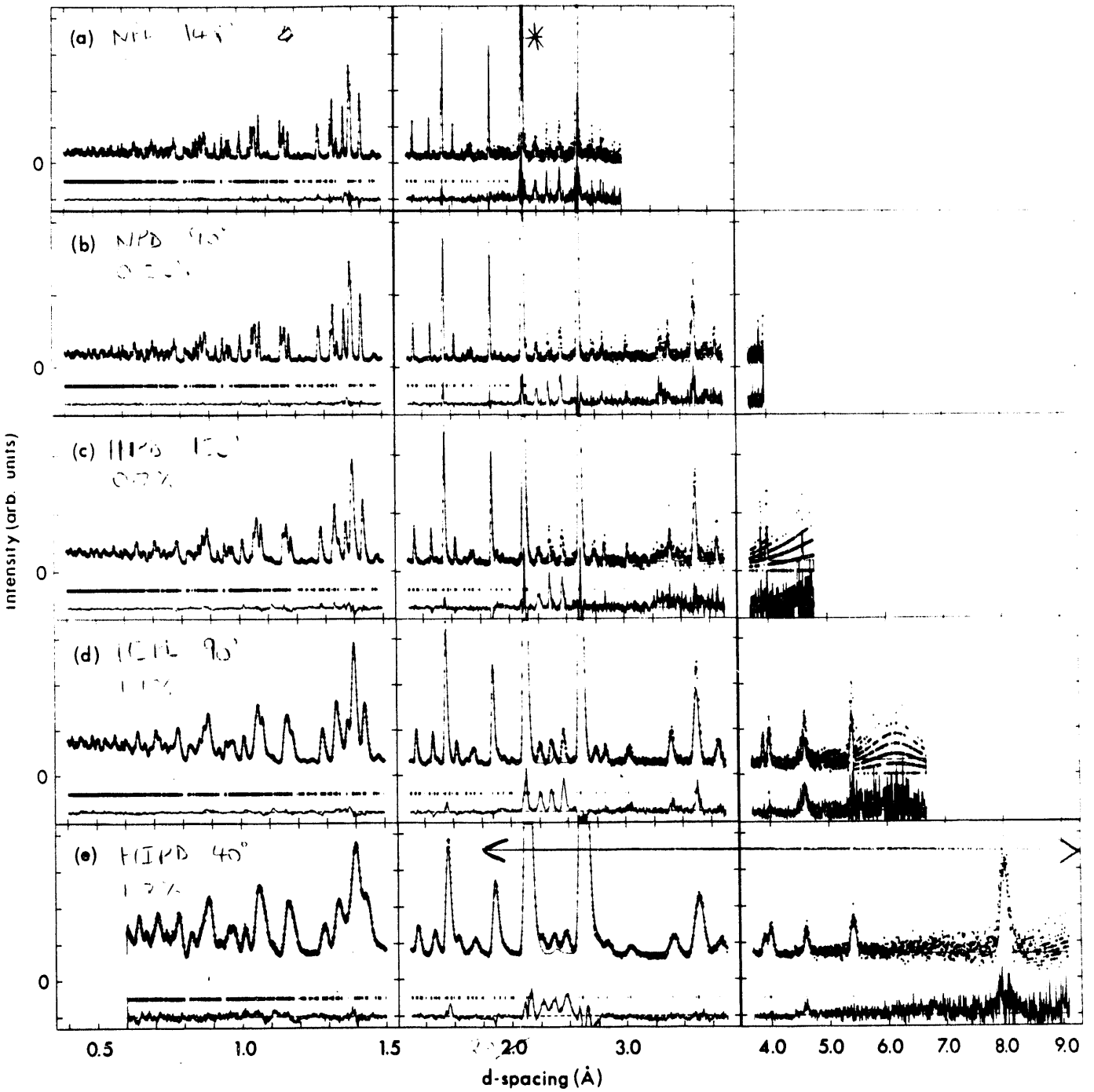
(a)
(b)
(c)
(d)
(e)
0
0
0
0
0
Intensity (arb. units)
0.5
1.0
1.5
2.0
3.0
4.0
5.0
6.0
7.0
8.0
9.0
d-spacing (Å)

DATE FILMED

9/7/94

END